Available online at www.sciencedirect.com
ScienceDirect
Journal of the European Ceramic Society 27 (2007) 1513–1520
www.elsevier.com/locate/jeurceramsoc

Experimental and numerical study of the thermomechanical behaviour of refractory model materials

Y. Joliff *, J. Absi, J.C. Glandus, M. Huger, N. Tessier-Doyen

GEMH, Ecole Nationale Supérieure de Céramique Industrielle, 47 à 73 avenue Albert Thomas, 87065 Limoges Cedex, France

Available online 22 May 2006

Abstract

The thermomechanical behaviour of refractory materials in use is strongly dependent on their Young's modulus value. However, their microstructural complexity makes difficult the understanding of the influence of temperature on elastic moduli and the use of simplified models is needed.

Consequently, two complementary analytical and numerical approaches coupled with experimental measurements on simplified bi-phased model materials (glass matrix surrounding mono-diametral spherical inclusions of alumina) were implemented.

The elastic behaviour of model materials involving perfect cohesive matrix/inclusions interfaces has been previously studied in the laboratory. So, the present work is focused on materials with partly cohesive matrix/inclusions interfaces. An ultrasonic technique was used to measure Young's modulus values and the finite element method (FEM) to perform numerical simulations. The experimental study of Young's modulus versus temperature shows a hysteresis loop characteristic of the interfaces closing and opening. Finally, a comparison of experimental and simulated results with those given by the most common analytical models was carried out.

Keywords: Refractories; Thermal expansion; Mechanical properties; Interfaces

1. Introduction

The heterogeneity of industrial refractory materials results from their multiphased composition involving aggregates of different sizes, bonding phases and various additives. The grains arrangement, the shape of aggregates and the microstructural defects such as porosity and cracks, make difficult the prediction of the mechanical and thermal behaviours of such materials. So, in order to understand the impact of the composition and the microstructure on their elastic properties, this work deals with the Young's modulus study versus temperature. This property has been chosen because, for refractory materials, it generally exhibits typical hysteresis loop when the temperature varies (Fig. 1a,[1] b,[2] c[3]). At room temperature (after firing), the weak modulus is due to the internal damage induced by thermal expansion mismatch that occurs during the cooling stage of elaboration. Then, when temperature increases, the material resorbs this initial damage because the residual stresses due to the thermal expansion mismatch decrease gradually: thus, this mechanism leads to a progressive Young's modulus increase. During cooling, the vitreous phase, which promotes damage cure at high temperature, solidifies and the material keeps high elastic properties. Below a given temperature, the residual stresses level imposed by cooling generates damage again: the Young's modulus decreases and reaches value close to its initial one.[4]

Few papers have been published dealing with the temperature dependence of Young's modulus. Studying stable materials which do not suffer any structural nor microstructural transformations, Wachtman et al.[5] showed in 1961 that a regular and reversible decrease is generally observed in the Young's modulus versus temperature plot, such a behaviour being imputed to the weakening of interatomic bondings. However, because of their coarse grains, heterogeneous and multiscaled structure, refractories exhibit behaviours far from this prediction and, indeed, research works rather report an hysteresis loop shape for Young's modulus variations versus temperature. For example, Case et al.[6] have observed hysteresis phenomena on anisotropic coarse grained alumina material and Nonnet et al.[7] so as Baudson et al.[8] have underlined similar behaviours for alumina castables and MgO/C refractories. These discrepancies, with the predictions given by the model of Wachtman et al.[5] are not always due to the same physical mechanisms. However most frequently they

* Corresponding author. Tel.: +33 5 5545 2222.
E-mail address: y_joliff@ensci.fr (Y. Joliff).

0955-2219/$ – see front matter © 2006 Elsevier Ltd. All rights reserved.
doi:10.1016/j.jeurceramsoc.2006.04.031

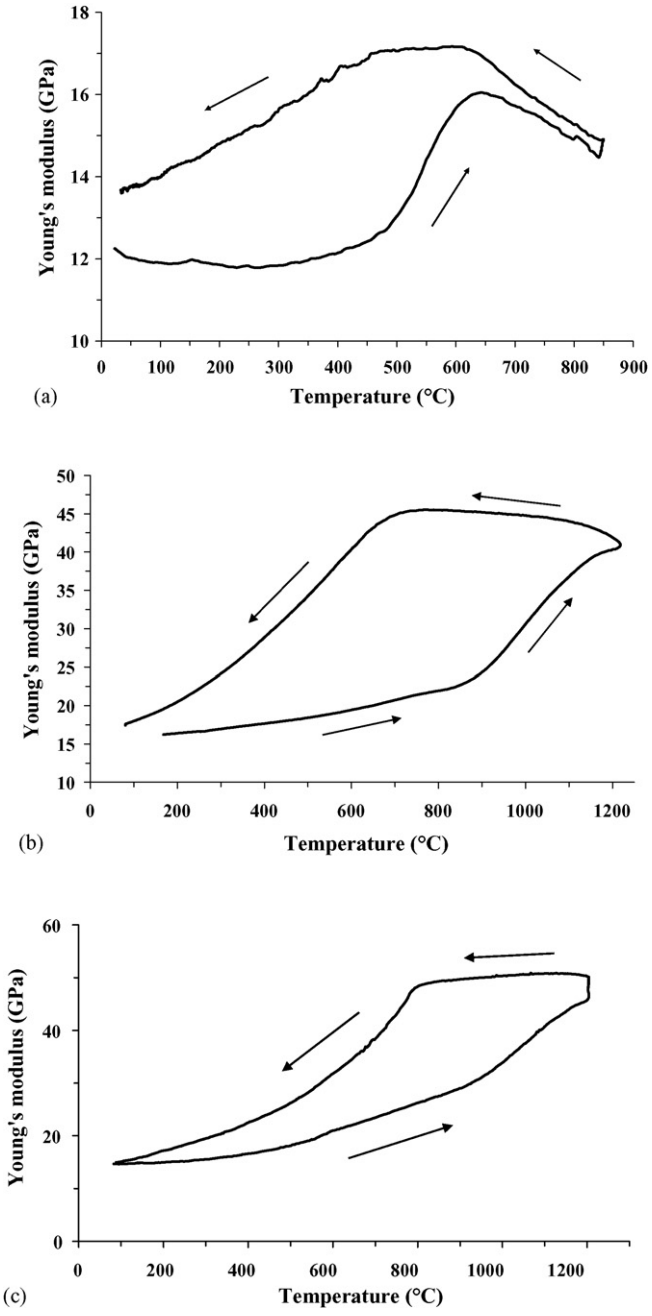

Fig. 1. Example of Young's modulus variations vs. temperature of refractories: (a) alumina/carbon[1]; (b) mullite/cordierite[2]; (c) andalusite concrete (second cycle).[3]

can be explained by the thermal expansion mismatch between the solid phases.

In order to understand the mechanical behaviour of real refractory materials, a first approach consists in simplify their microstructure. In this work, we study a heterogeneous model material composed of a glass matrix with alumina spherical inclusions. It makes possible to control the elaboration stage and to study the influence of a reduced number of parameters.

2. Elaboration of model materials

The material used for this work is a two-phased one, with mono-diameter spherical alumina balls within matrix of glass (Fig. 2). This matrix has been chosen because its coefficient of thermal expansion (CTE) directly depends on its oxides content. Two families of materials are studied. The samples of the first family, named cohesive model materials, exhibit a good CTE agreement between the matrix and inclusions ($\Delta\alpha = 0.2\text{E}{-6}\,\text{K}^{-1}$) and consequently a perfect cohesive interfaces. The samples of the second family, decohesive model materials, exhibit a CTE disagreement ($\Delta\alpha = 3\text{E}{-6}\,\text{K}^{-1}$) and a partly cohesive matrix/inclusions interfaces.

The glass frit is mixed with additives (water, methocel, peg300, acetic acid) which improve the plasticity and lubrication of the mixture.[4] The good content of alumina balls is then added to this mixture. After homogenization, the mixture is uniaxialy pressed (46 MPa) in a mould of 80 mm × 40 mm. The green material is then naturally sintered at 750 °C for the cohesive model samples and 860 °C for the decohesive model samples. In order to increase the densification, a post sintering stage at 790 °C under a 5 MPa pressure is performed. So, the final materials exhibit less than 2% of porosity. Table 1 shows the thermal and mechanical properties of each constituent.

3. Microstructure of decohesive model materials

In composite materials which exhibit a CTE disagreement between the matrix and inclusions, decohesions arise in zones where the stress level exceeds the material strength. Many analytical models[9–11] show that this zone is located at the matrix/inclusions interfaces, if these interfaces are free of interphases. The radial stress in the matrix can be expressed in the following form[12]:

$$\sigma_{rr}^{m} = \frac{1}{(r/r_0)^3}\,\frac{12G_m K_p(\alpha_m - \alpha_p)\Delta T}{4G_m + 3K_p} \tag{1}$$

where G_m, K_m, α_m, G_p, K_p and α_p, stand, respectively, for the shear modulus, bulk modulus and coefficient of thermal expansion for matrix and particles. ΔT represents the temperature difference between the initial and current times. Thus, the radial stress reaches its maximum value at the interface and decreases according to a r^{-1} law when the distance from the centre of inclusion increases. Indeed, according to these analytical approaches, many decohesions can be observed at the matrix/inclusion interfaces (Fig. 3a).

However, for the glass/alumina material here studied, unexpected cracks appear in the matrix, out of the matrix/inclusion interfaces (Fig. 3b). Similar observations were reported by other authors,[13] but the literature does not propose any explanation dealing with the origin of such shifted cracks. Tirosh et al.[14] in the mechanical study of a tensile test, finds that cracking can occur in the matrix, out of the inclusion/matrix interface (Fig. 4). Moreover, he proposes an analytical relationship to calculate this gap on the basis of the elastic properties of the two materials and

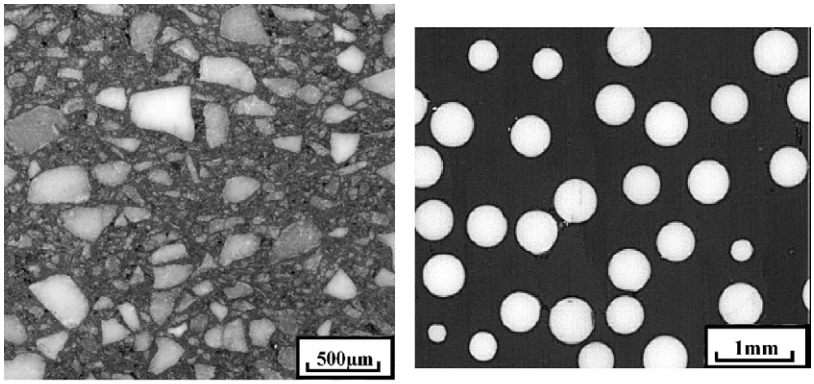

Fig. 2. Micrographs of an industrial refractory and of a simplified model material: (a) industrial refractory and (b) simplified model material.

Table 1
Thermal and mechanical properties of the constituents

	Designation	E (GPa)	ν	ρ (kg/m^3)	α (K^{-1})	C_p (J kg^{-1} K^{-1})	λ (W m^{-1} K^{-1})
Alumina	Brace 700 µm	340	0.24	3300	7.6E−6	868	25
Glass	Glass 1	76	0.21	2570	7.4E−6	838	1.4
Glass	Glass 2	68	0.206	2400	4.6E−6	838	0.98

the size of spherical inclusion:

$$\frac{\bar{r}}{R} = \sqrt{\frac{-6\delta}{2\beta + \gamma}} \tag{2}$$

r is the polar distance of the shifted crack, R the particle radius, δ, β and γ coefficients depending on E_m, E_p, ν_m and ν_p.

The numerical simulation of this test does not give similar results. Indeed, the finite elements calculation shows that the maximum stress level in the sample is located at the matrix/inclusion interface. So, cracks must be observed in this place only. This disagreement can perhaps be explained by the assumptions used by Tirosh but which are not described in the paper.

Micrographs of Fig. 3c show also that when two inclusions are close, an unexpected crack, whose length increases when the distance between inclusions decreases, develops halfway. Moreover, they show that no crack is observable out of the interface if inclusions are sufficiently far one to the others. Finally, It must be noticed that in all cases, a decohesion at the inclusion/matrix interface can be observed (Fig. 3a).

To understand the origin of these phenomena, numerical 3D models containing two spherical alumina inclusions in a parallelepipedic matrix of glass have been developed. The parametric variable of this study was the distance l between inclusions (Fig. 5). At the beginning of calculation, the sample is uniformly at the temperature of 860 °C. Then the model is cooled at 20 °C. The inclusions/matrix interfaces are supposed cohesive in order to induce stresses (Fig. 5). Four models named M1, M2, M3 and M4 were considered for respective l/d ratios of 1/3, 3/3, 5/3 and 7/3. Numerical models are built in 3D and 2D1/2. For M1 model, the results in 2D1/2 and 3D are perfectly similar so that

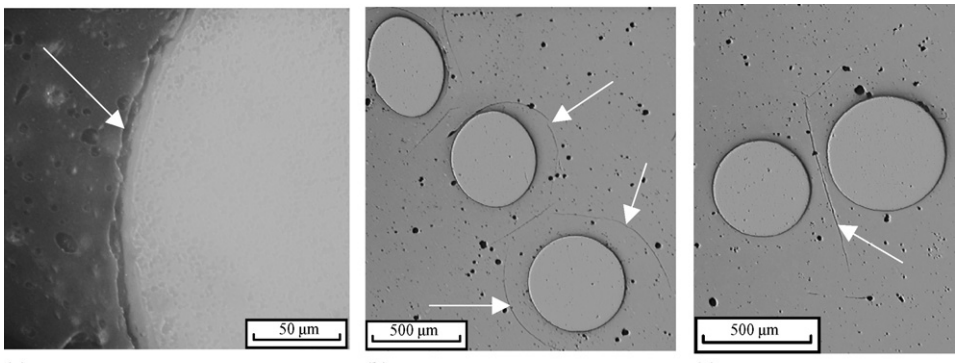

Fig. 3. Real model material with 20 vol.% of alumina: (a) interfacial debonding zone; (b) microcracks away from the interface; (c) microcrack between two close inclusions.

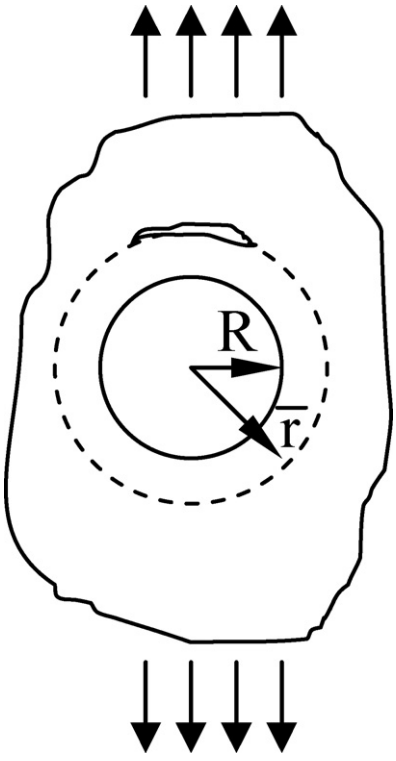

Fig. 4. Circumferential crack zone described by Tirosh et al.[14] in case of an applied tensile stress.

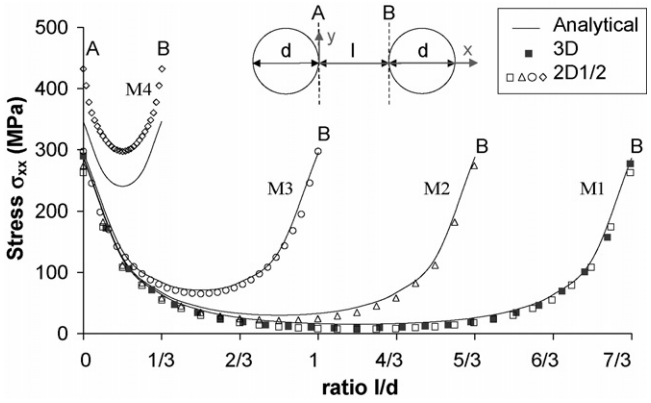

Fig. 6. Thermal stresses σ_{xx} in the matrix between two inclusions vs. *l*/*d* ratio.

it becomes justified to use the axisymmetric calculation for all the other models.

According to the results of analytical approaches, the numerical analysis show that the radial stress is always maximum at the inclusion/matrix interface (Fig. 6), but cannot allow to expect a shifted cracking, whatever the inter-inclusions distance *d* is. These results show also that the radial stress level increases when the inter-inclusions distance decreases. Such a result can justify the arising of cracking for the weakest inter-inclusions distances, but cannot account for its location halfway. Finally, it must be underlined that the weakness of the numerical models lies in the fact that they consider materials in solid state. So, they cannot take into account the progressive matrix transition from viscous

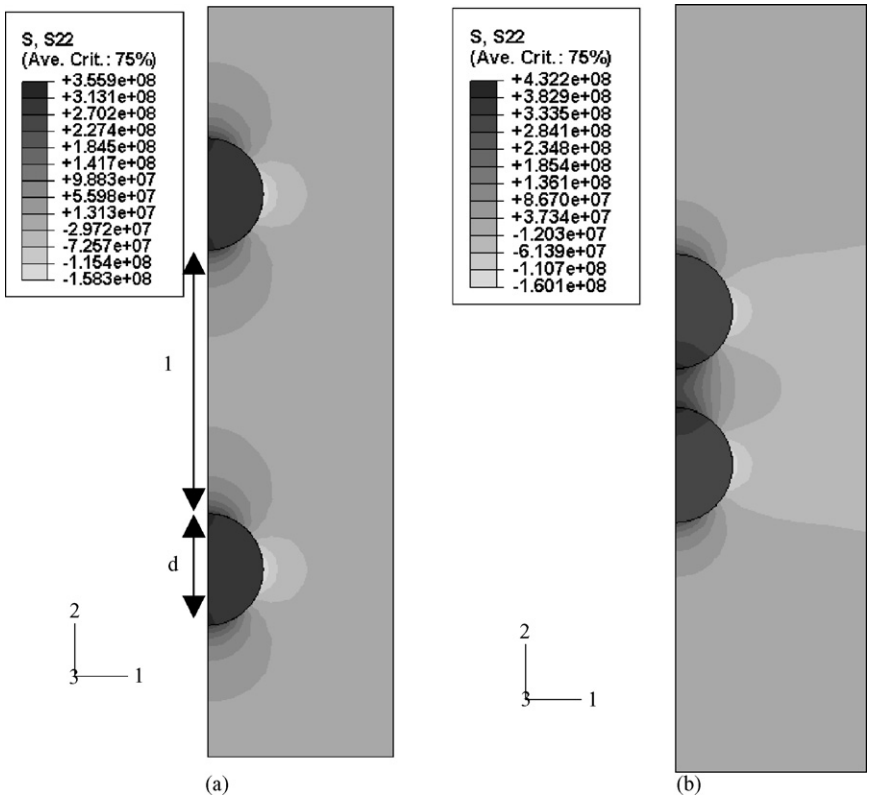

Fig. 5. Thermal stresses σ_{22} (Pa) for two numerical models: (a) M1 models and (b) M4 models.

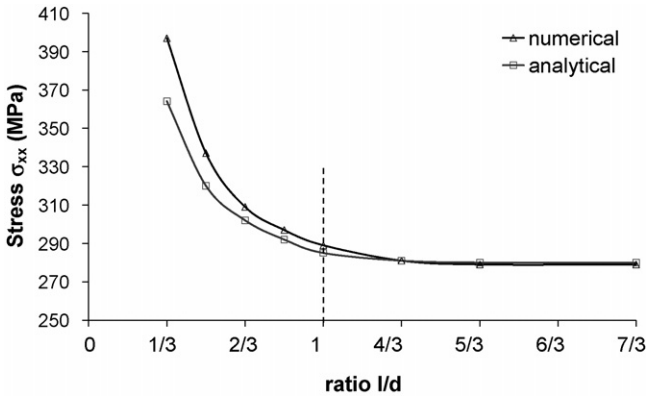

Fig. 7. Interfacial radial thermal stresses vs. *l*/*d* ratio.

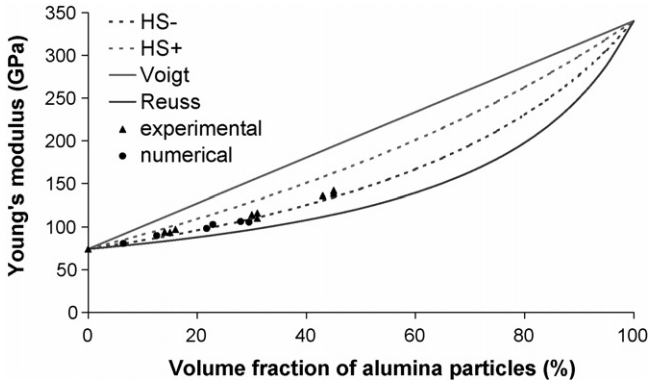

Fig. 8. Comparison between experimental, analytical and numerical Young's modulus values at room temperature for cohesive model materials.

to solid state. Fig. 7 represents the numerical radial stress values at the interface inclusions/matrix versus the *l*/*d* distance ratio. These stresses quickly increase when the distance between two inclusions is lower than the critical value 1. So, it can be thought that a critical state is reached when the inter-inclusions distance becomes lower than the inclusions diameter.

The difference between the numerical and analytical results can be explained by the simplifying assumptions used in the analytical model which postulates a constant stress level in the inclusions, whatever the inter-inclusions distance is. When inclusions are sufficiently far one from each other, this assumption is respected, but it is not when this distance becomes lower than the inclusion diameter. Indeed, in such cases, the numerical models show that the radial stress in the inclusions varies and that this variation increases when the inter-inclusions distance decreases because of the induced stress field disturbance (Fig. 5).

4. Elastic properties: experimental, analytical and numerical results

4.1. Room temperature Young's modulus

The most popular analytical model used to predict the elastic properties of a two-phased material is the Voigt[15] and Reuss[16] one because of its simplicity. However, the Hashin and Shtrikman[17] model which postulate a perfect contact between the matrix and spherical inclusions, is more stuited to our material (in case of good CTE agreement).

Young's modulus at room temperature is measured by an ultrasonic method in infinite medium with contact transducers.[18]

The results show the decohesion effects on the elastic properties of the material. The lower Hashin and Shtrikman[17] limit appears as well suited to describe the Young's modulus variations for cohesive model materials (Fig. 8), but it overestimates the elastic properties of decohesive ones (Fig. 9).

Results of numerical 3D models, with similar volumic contents in inclusions as those of the characterised materials, have been compared to the experimental and analytical ones.

Finite element model (FEM) simulation consists in simulating a pure tensile test on cylindrical samples containing mono-diametral spherical inclusions whose random distribution is obtained thanks to an original software developed in the laboratory in C++ language. Young's modulus of this two-phased materials is estimated by using Hooke's law.

Various models were studied whose volumic contents in inclusions vary from 6 to 30%. The cohesive model materials suppose a total and perfect contact between matrix and inclusions and thus the continuity of displacements at the interfaces. In the case of decohesive model materials, the contact matrix/inclusions is partial: in a first approach and, with the aim of numerical simplification, it was fixed at 50% of the outside inclusions surface. Finally, porous model materials were studied by giving the air properties to spherical inclusions:

- In the case of cohesive model materials Fig. 8 shows the very good agreement between the numerical and experimental results.
- For porous model materials, the numerical results agree with the upper Hashin and Shtrikman[17] limit.
- The experimental values dealing with decohesive materials lie between the lower Hashin and Shtrikman[17] limit for a cohesive model and its upper limit for a porous one.
- Finally, the numerical decohesive materials give results lower than the experimental values. This can be explained by the

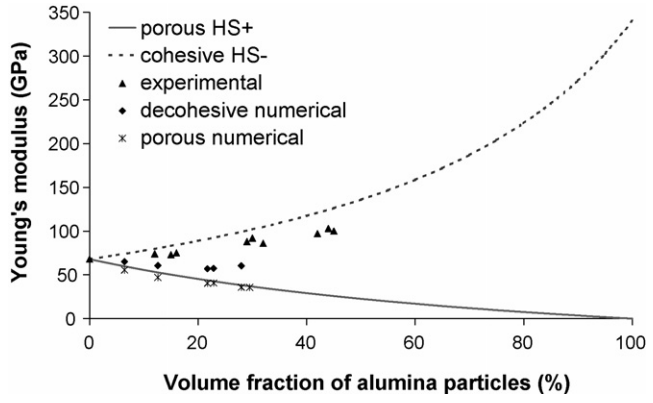

Fig. 9. Comparison between experimental, analytical and numerical Young's modulus values at room temperature for decohesive model materials.

extreme simplification used in this work for the zone of partial contact between the matrix and inclusions. However, it may be thought that an improved management of this contact will make it possible to obtain a better agreement between the experimental and numerical values.

4.2. Young's modulus temperature dependence

The Young's modulus evolutions during a thermal cycle are measured by an ultrasonic technique of echography working in "long bar mode".[19] In this technique, ultrasonic waves produced by a magnetostrictive transducer subjected to a magnetic field, propagate through the sample by means of an alumina wave guide. The electronic signal obtained is composed of a series of echoes of decreasing amplitudes, corresponding to the successive round trips within the two ends of the sample. The measurement of the time (τ) between two consecutive echoes allows to estimate the waves velocity and to calculate Young's modulus by means of the relationship:

$$E = \rho\left(\frac{2L}{\tau}\right)^2 \quad (3)$$

where L is the length of the sample and ρ is the material density.

The experimental results have been compared to the Hashin and Shtrikman[17] lower bound versus. temperature assuming that Poisson's ratio is not temperature dependent.[20,21]

4.2.1. Temperature behaviour of components

The temperature dependence of elastic properties, especially Young's modulus, was studied for each component separately. The spherical inclusion phase is constituted of more than 99.9% of pure alumina. Since Young's modulus measurement in temperature cannot be carried out with balls, an estimated value is obtained using a similar alumina bar. Fig. 10 shows that alumina exhibits a linear decrease up to 1200 °C, whereas G1 and G2 glasses exhibit limited variations below the vitreous transition temperature. Beyond these limits, the elastic properties strongly decrease. For each of these components, the evolution is reversible during a thermal cycle.

4.2.2. Materials with cohesive interfaces

A previous work on cohesive model materials[22] has shown that the model materials with CTE agreement between matrix and inclusions exhibit reversible Young's modulus variations when the temperature varies. This work has shown also that the same evolutions are observable when the temperature increases or decreases. The lower limit of Hashin and Shtrikman[17] gives a good estimation of the elastic properties variations versus temperature for cohesive model materials. Thus, this analytical model will be used also here to analyse experimental results on decohesive model materials.

4.2.3. Materials with partly decohesive interfaces

For decohesive model materials, the Young's modulus increases gradually from 300 to 550 °C then it remains constant. This increase is due to the cure of material: the interfacial decohesions close again due to the temperature rising. Then, for temperatures higher than the transition temperature of the matrix, Young's modulus falls down. At this stage, the viscous state of glass weakens the material elastic properties. During cooling, the modulus increases again because of the glass solidification. The stage of cooling is in rather good agreement with the predictions of Hashin and Shtrikman[17] lower limit in the high temperatures range, up to 300 °C (Fig. 11).

Below 300 °C, decohesions between inclusions and matrix appear, inducing a Young's modulus decrease. When the content in alumina inclusions increases, the hysteresis loops become more and more wide. The increase in the number of decohesive surfaces between inclusions and matrix can be considered as responsible of this result. In each case, experimental results in the first stage of cooling remain in good agreement with the lower limit of Hashin and Shtrikman's model.[17]

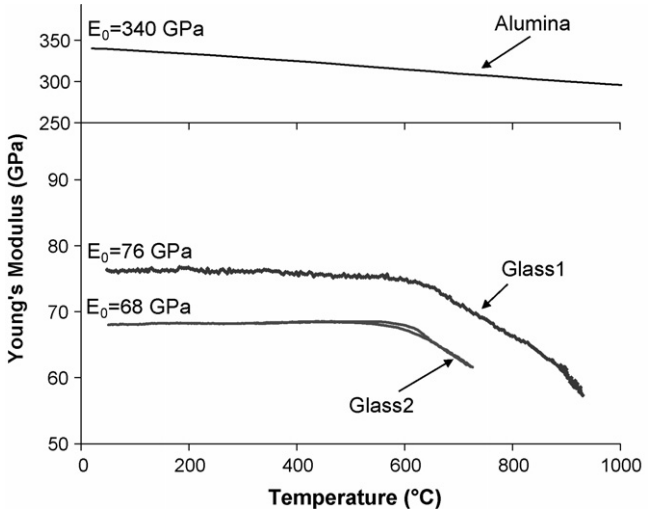

Fig. 10. Young's modulus of constituents vs. temperature.[22]

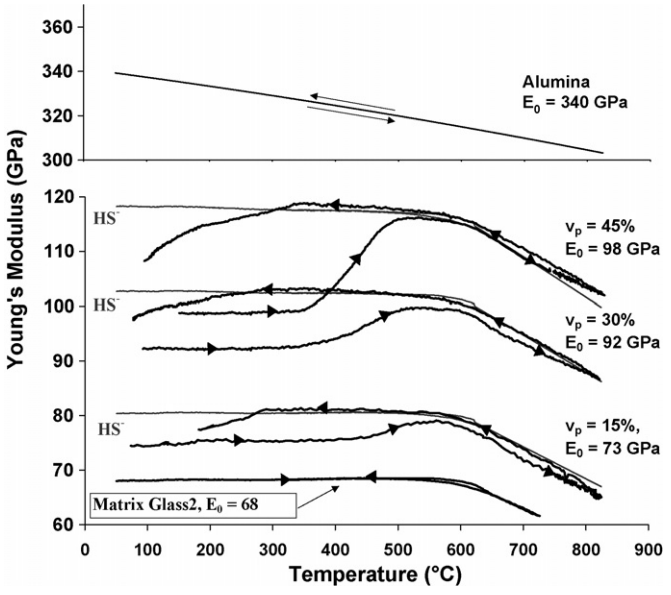

Fig. 11. Young's modulus vs. temperature for: alumina, Glass 2, and decohesive model materials containing 15, 30 and 45 vol.% of alumina inclusions.

5. Discussion

In spite of their very simplified microstructure including two phases only, the studied model materials allow realistic simulations of the behaviour of much more complex industrial refractory materials. However, the choice of a vitreous matrix, that is to say a not refractory material, can seem surprising. It has been made because the thermomechanical properties of such materials can be easily adjusted during the elaboration stage by modifying their oxides content. The measured evolutions of Young's modulus when the temperature varies prove that this choice is judicious.

Three methods (experimental, analytical and numerical) were used to study the Young's modulus of model materials, the experimental results being considered as the more pertinent because of their obvious physical significance. The literature is rich of examples[23–26] showing that the ultrasonic technique here used leads to results in perfect agreement with those given by other confident experimental methods. So, the measured values have been systematically taken as reference values for comparisons with analytical and numerical results.

In the case of materials exhibiting fully cohesive matrix/inclusions interfaces, the results obtained by using the analytical and numerical methods are identical to the measured values. This agreement validates the numerical model here developed and legitimates the use of the analytical Hashin and Shtrikman[17] analytical model, especially its lower limit well suited to materials composed of a compliant matrix surrounding rigid particles.

On the other hand, in the case of materials with decohesive interfaces, the lower limit of the Hashin and Shtrikman model[17] overestimates the Young's modulus values regarding the experimental results, because it is not able to take into account the material interfacial damages.

The numerical models developed to predict the Young's modulus values of materials exhibiting decohesive interfaces give a satisfactory description of the damage at the matrice/inclusions interfaces. However, they are built on arbitrary simplifying assumptions illustrated by Fig. 12:

- One-half of the peripheral surface of inclusions is supposed perfectly bonded to the matrix, the other half being decohesive.

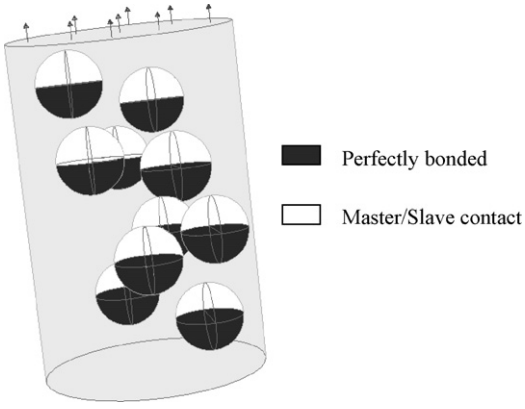

Fig. 12. Contact description: representative example used in numerical models.

- The axes of the free and bonded half-spheres are parallel to the axis of the cylindrical matrix.
- The external tensile loading is applied along this preferential direction.

This first approach shows only the ability of numerical tools to describe the behaviour of model materials with decohesive matrix/inclusions interfaces. A more rigorous numerical work will be published soon. In this next paper, more realistic assumptions are postulated and the most significant variables of the problem (importance of the decohesive surface at the interface, orientation of this interfacial damage zone . . .) are adjustable.

6. Conclusion

The complex thermomechanical behaviour of refractory materials is due to their heterogeneity and multiphased composition. During heat treatments, thermal expansion mismatches between the different phases may generate internal stresses that can damage the material.

The use of model materials with simplified microstructure (glass matrix with alumina spherical inclusions) is well suited to the study of Young's modulus versus temperature evolutions for materials exhibiting cohesive and decohesive matrix/inclusions interfaces. Experimental results have shown the impact of a decohesive state on elastic properties of the studied materials. Young's modulus curves exhibit hysteresis loops, typical of closing and opening microcracks mechanisms during heating and cooling, respectively.

Analytical models and numerical simulations have been used in order to predict these behaviours. The lower bound of the Hashin and Shtrikman model appears as well suited to predict the elastic properties of materials with cohesive interfaces. On the other hand, for materials with decohesive interfaces, analytical models cannot be used because they do not take into account microcracks around particles. In such cases, numerical approaches can account for the influence of decohesive interfaces on Young's modulus by using mechanical models assuming a partial contact between the matrix cavities and particles.

Acknowledgements

Yoann Joliff would like to express his gratitude towards the Limousin Region and the European Social Fund for financial support of the present work.

References

1. Vaudez, S., Huger, M. and Gault, C., Mechanical behaviour of Al_2O_3/C shaped refractories used in continuous casting. In *Proceedings 6th Ecers Conference. Vol 2*, 1999, pp. 159–160.
2. Soro, J., Bonnet, J. P. and Huger, M., Etude des propriétés physiques et thermomécaniques de matériaux réfractaires cordiérite/mullite. Internal Report. GEMH Laboratory, Limoges, France, 2005.
3. Yeugo Fogaing, E., Caractérisation à haute température des propriétés d'élasticité de refractaires électrofondus et de bétons réfractaires. Ph.D. Thesis. University of Limoges, France, 2006.

4. Tessier-Doyen, N., Etude expérimentale et numérique du comportement thermomécanique de matériaux réfractaires modèles. Ph.D. Thesis. University of Limoges, France, 2003.
5. Wachtman, J. B., Telft, W. E., Lam, D. G. and Apstein, C. S., Exponential temperature dependance of Young's modulus for several oxides. *Phys. Rev.*, 1961, **122**, 1754–1760.
6. Case, E. D., Smyth, J. R. and Hunter, O., Microcracking in large-grain Al_2O_3. *Mater. Sci. Eng.*, 1981, **51**, 175–179.
7. Nonnet, E., Lequeux, N. and Boch, P., Elastic properties of high alumina cement castables from room temperature to 1600 °C. *J. Eur. Ceram. Soc.*, 1999, **19**, 1575–1583.
8. Baudson, H., Debucquoy, F., Huger, M., Gault, C. and Rigaud, M., Ultrasonic measurement of Young's modulus MgO/C refractories at high temperature. *J. Eur. Ceram. Soc.*, 1999, **19**, 1895–1901.
9. Husueh, C. H., Becher, P. F. and Sun, E. Y., Analyses of thermal expansion behaviour of intergranular two-phase composites composites. *JMS*, 2001, **36**, 255–261.
10. Dean-Mo, L. and Jenny Winn, E., Microstresses in particulate-reinforced brittle composites. *JMS*, 2001, **36**, 3487–3495.
11. Hsueh, C. H. and Becher, P. F., Residual thermal stresses in ceramic composites. Part II: with short fibers. *Mater. Sci. Eng.*, 1996, **A212**, 29–35.
12. Lauke, B., Schüller, T. and Beckert, W., Calculation of adhesion strength at the interface of a coated particle embedded within matrix under multiaxial load. *Comput. Mater. Sci.*, 2000, **18**, 362–380.
13. Davidge, R. W. and Green, T. J., The strength of two-phase ceramic/glass materials. *JMS*, 1968, **3**, 629–634.
14. Tirosh, J., Nachlis, W. and Hunston, D., Strength behaviour of toughened polymers by fibrous (or particulate) elastomers. *Mech. Matér.*, 1995, **19**, 329–342.
15. Voigt, W., *Lehrbuch der Kristallphysik*. Teubner, Berlin, 1910.
16. Reuss, A., Berechnung der Fliessgrenze von mischkristallen auf Grund der plastizitätsbedingung für Einkristalle. *Z. Angew. Math. u. Mech.*, 1929, **9**, 49–58.
17. Hashin, Z. and Shtrikman, S., A variational approach to the theory of the elastic behavior of multiphase materials. *J. Mech. Phys. Solids*, 1963, **11**, 127–140.
18. Cutard, T., Fargeot, D., Gault, C. and Huger, M., Time delay and phase shift measurements for ultrasonic pulses using autocorrelation methods. *J. Appl. Phys.*, 1994, **75**, 1909–1913.
19. Huger, M., Fargeot, D. and Gault, C., High temperature measurement of ultrasonic wave velocity in refractory materials. *High Temp. High Pressure*, 2002, **34**, 193–201.
20. Sakaguchi, S., Murayama, N., Kodama, Y. and Wakai, F., The Poisson's ratio of engineering ceramics at elevated temperature. *J. Mater. Sci. Lett.*, 1991, **10**, 282–284.
21. Lemercier, H., Verres du Système Y-Si-Al-O-N: propriétés, structure et cristallisation. Ph.D. Thesis. University of Limoges, France, 1995.
22. Tessier-Doyen, N., Glandus, J. C. and Huger, M., Untypical Young's modulus evolution of model refractories at high temperature. *J. Eur. Ceram. Soc.*, 2006, **26**, 289–295.
23. Billy, M., Boch, P., Dumazeau, C. *et al.*, Preparation and properties of new silicon oxynotride based ceramics. *Ceram. Int.*, 1981, **7**(1), 13–18.
24. Fargeot, D., Glandus, J. C. and Boch, P., Constantes élastiques des alliages cuivre-aluminium riches en cuivre entre 77 et 293 K. *Phys. Stat. Sol. a*, 1976, **35**, 687–695.
25. Boch, P. and Glandus, J. C., Elastic properties of silicon oxynitride. *J. Mater. Sci.*, 1979, **14**, 379–385.
26. Glandus, J. C., Rupture fragile et résistance aux chocs thermiques de céramiques à usages mécaniques, Thèse d'Etat. University of Limoges, France, 1981.